Global and Directional Activation Maps for Cardiac Mapping in Electrophysiology

Rémi Dubois, Simon Labarthe, Yves Coudière, Mélèze Hocini, Michel Haïssaguerre

Global and Directional Activation Maps for Cardiac Mapping in Electrophysiology

R Dubois[1], S Labarthe[2], Y Coudière[2], M Hocini[1,3], M Haïssaguerre[1,3]

[1]LIRYC, Université de Bordeaux, F33600, Pessac, France, [2]Carmen, Inria, Talence, F33400, Bordeaux, France, [3]Hôpital Cardiologique du Haut Lévêque, F33600, Pessac, France.

Abstract

Cardiac mapping is a necessary step for accurate diagnostics in cardiology. It generates an activation map of the pathways followed by the electrical depolarization wavefront during the activity of the heart. In some cases, the standard methods to construct activation maps based on the derivatives of the signals may lead to inaccurate results.

In this paper, we evaluated a novel Directional Activation Algorithm (DAA) based on EGM analysis. The DAA calculates the time delays between adjacent EGMs and assigns to each a localized propagation vector. We propose a new visual representation of the depolarization wavefront as a field of arrows to facilitate comprehension of propagation pathways; and in addition, we show resultant global activation map.

The accuracy of the proposed methodology is compared with known activities obtained from a monodomain, isotrope, Beeler-Reuter model of the atria.

1. Introduction

Cardiac arrhythmia occurs when the electrical impulses propagate abnormally in the heart muscle. Typical examples are common flutters or focal tachycardia. During focal activity for example, abnormal depolarizations originating from a group of diseased cells propagate over the whole cavity, generating abnormal contractions.

Electrophysiology (EP) studies aim at studying the potentials from the heart for a thorough understanding of the propagation pathways [1]. The recordings (EGM) can be either recorded with catheter inside the heart, by epicardial socket of electrodes or derived from optical measurements in case of ex-vivo experiments.

Hitherto, limited EGM processing is being undertaken [1, 2] to extract common relevant features like 1) voltage mapping, in which the amplitude of the EGMs are analyzed to localize injured or scarred tissues, and 2) activation mapping, which studies the temporal intervals between activations by comparing the EGMs recorded simultaneously at several locations.

In a standard computation, the local activation time (LAT) at each location is estimated (Fig. 1). The LAT is defined as the time when the electrical wavefront passes beneath the electrode. It is usually set either at the maximum negative slope of the electrical deflection for unipolar EGMs, or at the maximum signal magnitude for bipolar recordings [3]. In many cases, this estimate can be wrong because of multiple negative deflections, fractionated electrograms or poor signal to noise ratio particularly in unipolar recordings [1, 4, 5]. As an alternative, some other features were proposed to mark the EGMs [6-9] but they exhibit a common flaw: each EGM is studied independently from the others.

This paper presents a new approach to analyze EGMs and to extract the propagation pathways. It leads to two complementary maps based on the same principle: the comparison of EGMs from neighboring locations (Fig. 2).

The first map is equivalent to the activation map commonly used for the diagnosis, but constructed from the local comparison of EGMs. The second map, named Directional Activation Map (DAM), exhibits the local

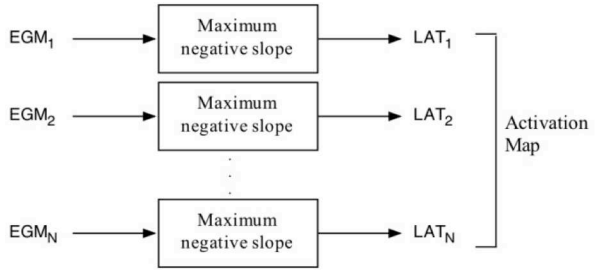

Fig. 1: The standard computation on unipolar EGMs to obtain an activation map is to estimate the Local Activation Time of each channel independently.

direction of activations based on the assumption of a locally plane depolarization wave. The next section of this paper is devoted to the mathematical basis of these two computations, and the method leading to the maps. The validation is based on the known activation pattern of the atria.

2. Methods

The core of the proposed methodology is the measurement of the delay in the activations of two neighboring locations during a single propagation of the depolarization wavefront (Fig. 2). The main advantage of using neighboring locations is that the similarity between their shapes of their EGMs permits their comparison

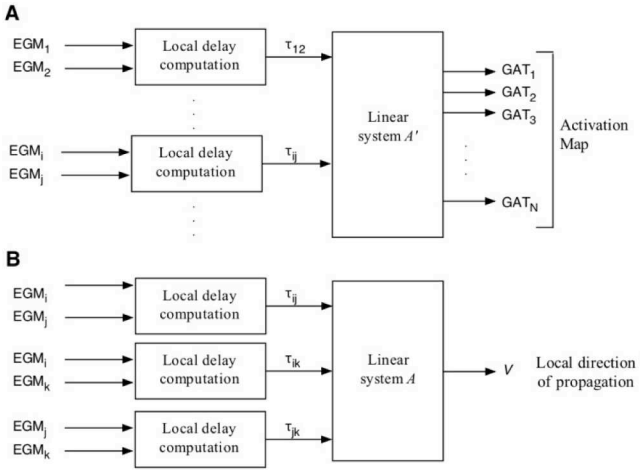

Fig. 2: From each couple of neighboring locations, a delay is estimated between the corresponding EGMs. These delays are the inputs for linear systems of equations that lead to the global activation map (A) and to the local direction of propagation (B).

without explicitly computing the LAT of each of them.

Global activation time (GAT)

This section lays the basis of the methodology used to compute a surrogate of the local activation time: the global activation time (GAT). Similar to LAT, GAT is an estimation of the time when the wavefront passes beneath each electrode; however, this estimation is global in the sense that it is computed in order to optimally fit the delays between EGMs recorded at all locations.

Let us assume N electrodes for which the activation map has to be computed. The GATs of two electrodes i and j are such that the difference is equal to the time necessary for the wavefront to travel from one to the other:

$$T_j - T_i = \tau_{ij} \qquad i,j = 1..N \;;\; i > j \tag{1}$$

Such equations are written for each pair of electrodes, the resulting system contains as many equations as the number of pairs of electrodes (N_e), and N unknowns. The matrix form is:

$$\mathbf{D}^T\mathbf{T} = \mathbf{t} \tag{2}$$

where $\mathbf{T} = [T_1,\ldots, T_N]^T$ is the vector of unknowns and $\mathbf{t} = [\{\tau_{ij}\}]$ is the vector of delays for each pair.

The general solution for $\mathbf{T}$ is:

$$\mathbf{T} = \mathbf{T_p} + \mathbf{T_N} \tag{3}$$

where $\mathbf{T_N}$ is any vector of the null space of $\mathbf{D}^T$, and $\mathbf{T_P}$ is given by:

$$\mathbf{T_p} = \tilde{\mathbf{T}} = (\mathbf{D}\mathbf{D}^T)^{-1}\mathbf{D}\mathbf{t} \tag{4}$$

In an ideal case, when the system (2) is consistent (ie when the rank of $\mathbf{D^T}$ is equal to the rank of the augmented matrix $[\mathbf{D^T}|\mathbf{t}]$), the solution $\tilde{\mathbf{T}}$ is exact, otherwise, $\tilde{\mathbf{T}}$ is the best solution for (2) in the least squares sense. Due to the property of $\mathbf{D^T}$, it can be shown that $\mathbf{T_N}$ is of dimension 1 and represents the time zero. In practice, $\mathbf{T_N}$ is set equal to $\min_i(\{\tilde{T}_i\})$ so that the time origin is set to the location which is first to activate.

Directional Activation Map (DAM)

In this section a more local view of the propagation is proposed, which leads to a new representation of the local activation (Fig. 2B). Here, the propagation of the electrical wavefront is modeled as that of a plane wave in a homogenous medium (Fig. 3). This model is strongly suggested by the fiber orientation of the cardiac tissue; moreover, it is certainly a valid approximation for measurements performed at close locations.

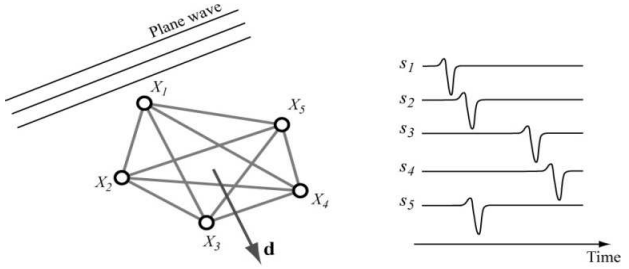

Fig. 3. Plane wave propagating in a tissue, and corresponding recorded EGMs in 5 locations. The estimation of the activation vector **d** is made from these measurements.

Let $\mathbf{x}_1$, $\mathbf{x}_2$, $\mathbf{x}_3$…, $\mathbf{x}_L$ be the locations in space of L neighboring electrodes. Let $\mathbf{n}$ be the unitary vector orthogonal to the wavefront plane; and $\mathbf{d}$ be the activation vector, defined as the vector orthogonal to the wavefront plane whose norm is inversely equal to the velocity v of the wave (Fig. 3). One has:

$$\mathbf{d} = \frac{1}{v}\mathbf{n} \tag{5}$$

Under the proposed assumption, the velocity v can be expressed as a function of the delay of activation of each of the electrodes in a pair $\mathbf{x}_i$ and $\mathbf{x}_j$ and the Euclidian distance between them:

$$v = \frac{(\mathbf{x_j} - \mathbf{x_i}).\mathbf{n}}{\tau_{ij}} \qquad (i,j) = 1..L, j > i \tag{6}$$

Thus a system of N_e equations – where N_e is the number of pair of electrodes – and its matrix form (8) is derived

$$(\mathbf{x}_j - \mathbf{x}_i).\mathbf{d} = \tau_{ij} \qquad (i,j) = 1..L, j > i \tag{7}$$

$$\mathbf{A}^T\mathbf{d} = \mathbf{t} \tag{8}$$

$\mathbf{A}$ is the $(3,N_e)$ matrix whose columns are the components of the N_e vectors $\mathbf{x}_j$–$\mathbf{x}_i$, and $\mathbf{t} = [\{\tau_{ij}\}]^T$ is the vector whose components are the N_e delays defined in (1). The general solution for the unknown $\mathbf{d}$ (ie the 3 coordinates

of the vector **d** in space) is given by:

$$\mathbf{d} = \mathbf{d_p} + \mathbf{d_N} \quad (9)$$

where $\mathbf{d_p} = \tilde{\mathbf{d}} = (\mathbf{A}\mathbf{A}^T)^{-1}\mathbf{A}\mathbf{t}$ (10)

and $\mathbf{d_N}$ is any vector of the null space of $\mathbf{A}^T$.

In an ideal case, when the propagation assumptions are true and the delays are measured without error, the solution $\tilde{\mathbf{d}}$ is unique and exact, and the null space of $\mathbf{A}^T$ is zero if $L \geq 3$ (and the 3 locations are not aligned). In practice, the plane propagation assumption is not met, and the delays measured between the locations are affected by noise, so that the system solution $\tilde{\mathbf{d}}$ is the best solution for (8) in the least squares sense.

For diagnosis, the method can be applied advantageously to the determination of a vector field of activation vectors for multiple electrode arrays. The Delaunay mesh delineation of the locations of measurements can be constructed and the system (8) can be solved for each elementary triangle. In that case, each system has N_e=3 equations (one equation per edge of the triangle) and only 2 unknowns that are the coordinates of the vector **d**, pertaining to the triangle, in the plane of the latter leading to Directional Activation Maps (DAM).

3 Results

The validation of the proposed methodology was estimated on simulated data according to three pathological scenarios: (1) a line of block in the roof of the left atrium, simulated with a null source function; (2) a scare zone closed to the mitral valve, modeled with a small conduction parameter to slow down the wave (3) an ectopic stimulation applied in a pulmonary vein.

The transmembrane potentials were computed with a monodomaine, isotrope, Beeler-Reuter model on atria segmented from CT-scan [10]. Then, unipolar EGMs were recovered from the simulations with a post-processing formula to simulate the electrode recordings.

Propagation Patterns

First, the global activation maps (GAM), and the directional activation maps (DAM) were validated on noise-free data. In each of the three scenarios, the diagnostic made from the computed maps was correct. Figure 4 shows the GAM for the ectopic activation. It exhibits the location of the focal source in the left inferior pulmonary vein as expected. Figure 5B shows the velocity map computed from the DAM. This map shows that the slow conduction area is well localized by the proposed computation of the velocity (see eq. 6). Figure 6 represents the DAM computed for scenario (1); in a normal propagation pattern, the wavefront should spread from the right pulmonary veins to the left pulmonary veins; but here, the arrows show that the propagation turn around the line of block in its lower side, and come back up on both sides of the line; which is correct in this case.

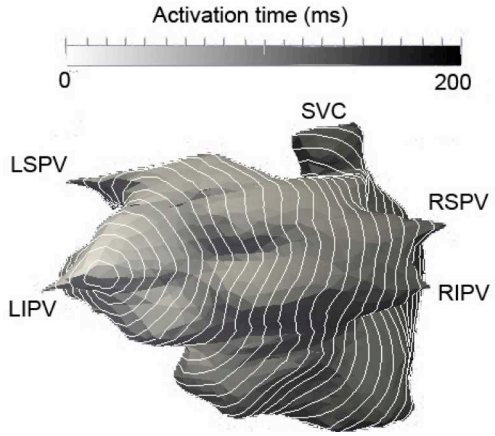

Fig. 4: The standard computation on unipolar EGMs to obtain an activation map is to estimate the Local Activation Time of each channel independently.

Activation Time

The validation was then performed against the standard algorithm with respect to the transmembrane potentials used as a gold standard. The mean value and the standard deviation of the error are reported Table I. For each scenario, various levels of white noise were added to estimate the accuracy of the algorithm with respect to noise.

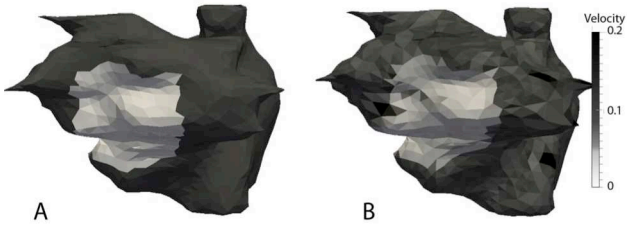

Fig. 5: (A) Post-Anterior view of the atria. The light grey localizes the area of slow conduction as set in the model. (B) Velocity map computed from the DAM.

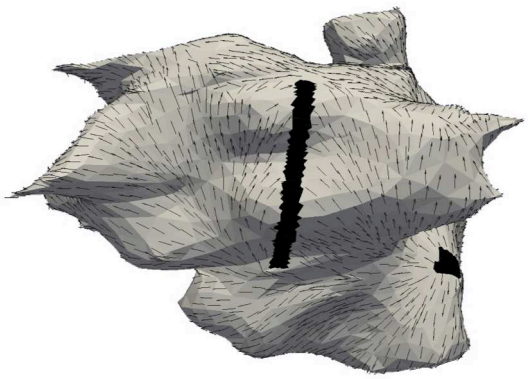

Fig. 6: DAM for line of block scenario, Post-Anterior view of the atria. The dark line is the line of block as set in the model. The arrows represent the local direction of propagation.

TABLE I
RESULTS FOR 3 SIMULATED HEART DISEASES

	Standard algorithm		**DAA Algorithm**	
	Mean (ms)	*Std (ms)*	*Mean (ms)*	*Std (ms)*
Line of block				
5%	0.00	8.84	-0.97	14.7
10%	0.12	12.2	-0.72	14.8
15%	4.30	36.8	2.81	16.9
20%	27.2	87.8	2.51	25.8
Scare tissue				
5%	-0.07	0.40	-0.07	0.50
10%	-0.08	0.44	-0.09	1.30
15%	0.46	10.8	0.45	3.19
20%	7.4	38.6	7.4	10.8
Focal activity				
5%	0.00	0.16	0.00	0.27
10%	0.04	1.80	0.04	0.81
15%	0.57	9.94	0.57	2.94
20%	6.17	37.7	6.27	11.1

Table I: Errors between the transmembrane depolarization and the activation time estimated from unipolar signals over 3 simulated heart diseases for various level of noise.

The results show that the accuracy of the proposed method is in the same range as that of the standard algorithm when the level of noise is low (5% and 10% of the signal range); but for noisy signals, the standard deviation of the error for the derivative based algorithm is quite large, when compared with the value obtained by the proposed method (around 3 times higher).

4. Conclusion

The activation map is an essential tool for diagnosis; it allows understanding the cardiac impulse conduction pathways. In this paper, we propose a new methodology to construct such maps, based on the comparison of EGMs recorded at neighboring locations rather than on the analysis of individual EGMs. The resulting activation maps led to the correct diagnosis in the three-tested scenarios. Moreover, it accuracy was preserved when the signals were noisy.

To date, focal, scar, and line of block have been investigated, and many other pathologies will be tested to validate the methodology. The applications of such novel method in Electrocardiographic Imaging or optical mapping could enhance performances.

Acknowledgements

This work was partially supported by an ANR grant part of “Investissements d’Avenir” program reference ANR-10-IAHU-04.

References

[1] Z. F. Issa, J. M. Miiler, and D. P. Zipes, *Clinical Arrhythmology and Electrophysiology*. Philadelphia, PA: Saunders, 2009.

[2] M. Shenasa, M. Borggrefe, and G. Breithardt, *Cardiac Mapping*: Futura Publishing Compagny, 1993.

[3] M. S. Spach, W. T. Miller, 3rd, E. Miller-Jones, R. B. Warren, and R. C. Barr, "Extracellular potentials related to intracellular action potentials during impulse conduction in anisotropic canine cardiac muscle," *Circ Res,* vol. 45, pp. 188-204, Aug 1979.

[4] M. S. Fuller, G. Sandor, B. Punske, B. Taccardi, R. S. MacLeod, P. R. Ershler, L. S. Green, and R. L. Lux, "Estimates of repolarization dispersion from electrocardiographic measurements," *Circulation,* vol. 102, pp. 685-91, Aug 8 2000.

[5] R. Plonsey and R. C. Barr, *Bioelectricity: A quantitative approach*: Springer, 2007.

[6] G. Ndrepepa, E. B. Caref, H. Yin, N. el-Sherif, and M. Restivo, "Activation time determination by high-resolution unipolar and bipolar extracellular electrograms in the canine heart," *J Cardiovasc Electrophysiol,* vol. 6, pp. 174-88, Mar 1995.

[7] C. F. Pieper, R. Blue, and A. Pacifico, "Simultaneously Collected Monopolar and Discrete Bipolar Electrograms: Comparison of Activation Time Detection Algorithms," *Pacing and Clinical Electrophysiology,* vol. 16, pp. 426-433, 1993.

[8] W. S. Ellis, S. J. Eisenberg, D. M. Auslender, M. W. Dae, A. Zakhor, and M. D. Lesh, *Deconvolution : A novel signal processing approach for determining activation time from fractionated electrograms and detecting infarcted tissue* vol. 94. Hagerstown, MD, ETATS-UNIS: Lippincott Williams & Wilkins, 1996.

[9] C. Cabo, J. M. Wharton, P. D. Wolf, R. E. Ideker, and W. M. Smith, "Activation in unipolar cardiac electrograms: a frequency analysis," *IEEE Trans Biomed Eng,* vol. 37, pp. 500-8, May 1990.

[10] G. W. Beeler and H. Reuter, "Reconstruction of the action potential of ventricular myocardial fibres," *The Journal of physiology,* vol. 268, pp. 177-210, Jun 1977.

Address for correspondence
Rémi Dubois, remi.dubois@espci.fr